INTERNATIONAL SOCIETY FOR
SOIL MECHANICS AND
GEOTECHNICAL ENGINEERING

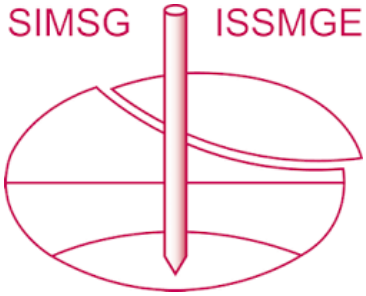

This paper was downloaded from the Online Library of the International Society for Soil Mechanics and Geotechnical Engineering (ISSMGE). The library is available here:

https://www.issmge.org/publications/online-library

This is an open-access database that archives thousands of papers published under the Auspices of the ISSMGE and maintained by the Innovation and Development Committee of ISSMGE.

Numerical analysis of settlements related to tunnelling: the role of stress-induced anisotropy and structure degradation in fine-grained soils

A. Amorosi
Technical University of Bari, Italy

D. Boldini
National Research Council and University of Rome "La Sapienza", Italy

ABSTRACT: In this paper numerical predictions of settlements induced by tunnelling in fine-grained soils are presented. The numerical analyses are aimed at separately establishing the relevance of stress-induced anisotropy and that of the structure degradation processes by adopting a constitutive model recently implemented in the finite element code Plaxis. The analysis of the results indicates that no significant influence of the considered aspects is relevant for tunnel induced ground settlements for volume losses which are typical of EPB or slurry shield tunnelling.

1 INTRODUCTION

Numerical predictions of settlements induced by tunnelling in fine grained soils are influenced by different factors, including 2D or 3D geometrical discretization, correct representation of the construction stages, assumed drainage conditions, numerical techniques and constitutive assumptions. The latter factor has been extensively investigated in recent years and a number of constitutive models have been adopted exploring their influence on the prediction of settlements. In this context, some Authors have highlighted the possible influence of elastic anisotropy on the deformation patterns obtained by Finite Element and Finite Difference analyses based on hardening plasticity material hypotheses (e.g.: Lee & Rowe, 1990; Simpson, 1996; Einav & Puzrin, 2004). Besides this aspect, bond degradation has been found to play a major role in the evolution of the mechanical behaviour of soft clayey soils and, as such, might influence the predicted subsidence induced by an excavation when a significant volume of soil undergoes plastic strains.

In this paper a set of 2D FEM simulations of the excavation of an ideal shallow tunnel in soft soil is presented. The numerical analyses are aimed at separately establishing the relevance of the stress-induced anisotropy and that of the de-structuring processes on the tunnelling induced ground deformation for free field conditions. The numerical results of this ideal problem are also compared to those obtained by well established empirical solutions.

2 CONSTITUTIVE MODEL FOR SOFT CLAY

The constitutive model is formulated in the framework of classical rate-independent plasticity. The reversible behaviour is described by a hyperelastic formulation originally proposed by Houlsby (1985) and modified by Borja, Tamagnini & Amorosi (1997), to include the elastic stiffness dependence on effective stresses; the elastic strain energy function is the following:

$$\Psi(\varepsilon_v^e,\varepsilon_s^e) = p_0\tilde{k}\,exp\left(\frac{\varepsilon_v^e - \varepsilon_{v0}^e}{\tilde{k}}\right) + \frac{3}{2}\left[\mu_0 + \alpha\, p_0\, exp\left(\frac{\varepsilon_v^e - \varepsilon_{v0}^e}{\tilde{k}}\right)\right](\varepsilon_s^e)^2 \quad (1)$$

where ε_{v0}^e is the elastic volumetric strain corresponding to the mean stress p_0, which is here set $= 0$ for $p_0 = 1$ kPa, $\tilde{k}$ is the elastic compressibility index and μ_0 and α are parameters. Under triaxial stress conditions for $\mu_0 > 0$ and $\alpha = 0$ the formulation results in a bulk modulus K dependent on p (mean pressure) and a constant shear modulus G, while for $\alpha > 0$ both nominal K and G depend on p and q (deviatoric stress). In this latter case the stiffness matrix is characterised by non-zero off-diagonal terms. As a consequence of this stress-induced anisotropy, the model predicts curved (parabola shaped) undrained stress paths. These features act similarly under the plane strain conditions adopted in the numerical analyses, leading to anisotropic elastic response for

Copyright © 2006 Taylor & Francis Group plc, London, UK

anisotropic stress states. The elastic stiffness matrix result:

$$\mathbf{D}^e := \frac{\partial^2 \Psi}{\partial \boldsymbol{\varepsilon}^e \otimes \partial \boldsymbol{\varepsilon}^e} = \frac{\left[1 + \frac{3}{2}\frac{\alpha}{\tilde{k}}\left(\varepsilon_s^e\right)^2\right]}{\tilde{k}} exp\left(\frac{\varepsilon_v^e}{\tilde{k}}\right)\mathbf{1}\otimes\mathbf{1} +$$

$$+2\left[\mu_0 + \alpha\, exp\left(\frac{\varepsilon_v^e}{\tilde{k}}\right)\right]\left[\mathbf{I} - \frac{1}{3}\mathbf{1}\otimes\mathbf{1}\right] + \frac{2\alpha}{\tilde{k}} exp\left(\frac{\varepsilon_v^e}{\tilde{k}}\left[\mathbf{1}\otimes\mathbf{e}^e + \mathbf{e}^e\otimes\mathbf{1}\right]\right) \tag{2}$$

The elastic domain is defined by the convex set $E_\sigma\{(\boldsymbol{\sigma}, p_c) | f(\boldsymbol{\sigma}, p_c) \le 0\}$, where f is the Modified Cam-Clay (MCC) yield function:

$$f(\boldsymbol{\sigma}, p_c) = \frac{q^2}{M^2} + p(p - p_c) \tag{3}$$

The isotropic hardening law is a modified version of that originally proposed by Kavvadas & Amorosi (2000) in their Model for Structured Soils (MSS):

$$\dot{p}_c = p_c\left[\frac{1}{\tilde{\lambda} - \tilde{\kappa}}\dot{\varepsilon}_v^p - \xi_v\, exp(-\eta_v \varepsilon_v^d)\dot{\varepsilon}_v^d - \xi_s\, exp(-\eta_s \varepsilon_s^p)\dot{\varepsilon}_s^p\right] \tag{4}$$

It is composed by two volumetric terms and a deviatoric one. The first volumetric term is similar to the standard MCC hardening law, here defined with reference to a bilogarithmic compressibility plot characterized by the parameters $\tilde{\lambda}$ and $\tilde{k}$. The following terms account for the volumetric and deviatoric strain-induced structure degradation by means of two separate exponential damage-type forms, in which the parameters ξ_v, η_v, ξ_s, η_s control the intensity and the rate of the phenomena. The major difference between this hardening rule and that formulated in MSS consists in the use of an increasing function of the volumetric plastic strain as controlling variable for the volumetric strain induced destructuring, defined as:

$$\varepsilon_v^d = \int_0^t \left|\dot{\varepsilon}_v^p\right| dt \tag{5}$$

The numerical integration of the constitutive model is performed by an algorithmical scheme which belongs to the class of the Generalized Backward Euler method. It has been adopted to ensure that, even in presence of strongly non linear irreversible response, the solution would be first-order accurate and numerically stable (Ortiz & Popov, 1985). Further details are given in Amorosi & Boldini (2003).

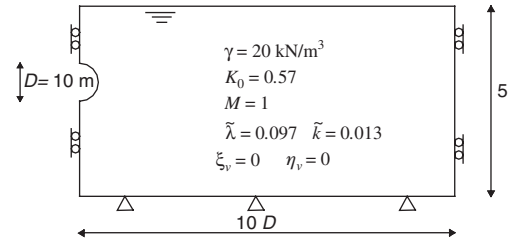

Figure 1. Geometry of the problem and soil parameters adopted for all the numerical analyses.

3 NUMERICAL ANALYSES

3.1 *Geometry, boundary and initial conditions, modelling of the excavation*

The geometry of the numerical model is shown in Figure 1. The coordinate system is defined such that x is the distance from the tunnel axis in the horizontal direction and z is the depth below the ground surface. The tunnel is located at a depth of $z_0 = 20$ m and is characterized by a diameter $D = 10$ m. It is excavated in a homogeneous layer of soft clay with the ground water level coincident to the ground level. The value of K_0 is selected according to the expression proposed by Jâky (1944) for normally consolidated clays.

All the analyses are performed in undrained conditions. Modelling of initial structure is obtained by increasing the preconsolidation pressure of the material with depth by means of the negative exponential function:

$$\Delta p_c = \Delta p_c(z=0) exp^{-\omega \cdot z} \tag{6}$$

where $\Delta p_c(z=0)$ is the increment of preconsolidation pressure at the ground surface, set equal to 200 kPa for $\omega = 0.015$.

The numerical study is performed by the Finite Element Program Plaxis, where the previously described constitutive model has recently been implemented (Amorosi et al., 2004). The mesh is composed by 15-node triangular plain strain elements. The excavation of the tunnel was simulated by de-activating the soil elements inside the tunnel section, by replacing these elements with equivalent nodal forces at the tunnel boundaries and by progressively reducing these nodal forces to simulate the tunnel face advancement.

In the numerical analyses the reduction of the nodal forces was performed by imposing decrements equal or lower than 2%.

3.2 *Aim of the numerical study*

The two series of numerical analyses A and B were carried out to investigate the role of the stress-induced anisotropy. In analysis A the single stratum of clay

Copyright © 2006 Taylor & Francis Group plc, London, UK

Table 1. Mechanical parameters for soft clay.

Analysis	A	B	C1	C2	C3	C4
α	178	0	178	178	178	178
μ_0	0	variable	0	0	0	0
ξ_s	0	0	10	20	30	40
η_s	0	0	10	20	30	40

is characterised by the elastic parameters $\mu_0 = 0$ and $\alpha > 0$. This influences both the initial elastic stiffness and the elastic response during the excavation. For the initial K_0 anisotropic stress state the adopted hyperelastic formulation predicts variable stiffness with depth and, at the same depth, different stiffness along the vertical and horizontal axes (nominally $Ev/Eh = 1.33$). During the excavation stages the elastic stiffness and its degree of anisotropy evolve all over the mesh as a consequence of the varying intensity of the stress tensor and orientation of its principal directions.

The results of this analysis are compared to those obtained by analysis B, in which the clay stratum is sub-divided into 20 thin strata, all characterised by the elastic parameters $\mu_0 > 0$ and $\alpha = 0$, with μ_0 linearly increasing with depth. In this case stress-induced anisotropy is neglected throughout the analysis and the stiffness matrix at every depth is characterised by an isotropic structure with $G = \mu_0 = \text{constant}$. To render comparable analysis B to A, appropriate values of the elastic parameter μ_0 were adopted for each substratum to fit the initial shear stiffness assumed at the same depth in the analysis A.

In both series of analyses A and B the plastic hardening parameters were selected in order not to simulate de-structuring processes (i.e. a Modified Cam-Clay behaviour was assumed for the plastic regime). Analyses C1-4 were carried out to establish the influence of the plastic strain-driven structure degradation phenomena on the predicted settlement troughs. In these cases the reversible response coincides with that assumed in analysis A while the deviatoric degradation parameters ξ_s, η_s are activated with increasing intensity from C1 to C4.

3.3 *Soil parameters*

Table 1 shows the values of the parameters adopted in the analyses. The hyperelastic parameter $\tilde{\kappa}$ was selected with reference to the typical values of the initial slope of the swelling lines observed in natural clay samples subjected to isotropic unloading and plotted in a bi-log compressibility plane. The hyperelastic parameter α was defined as follows: the very small strain shear stiffness modulus G_0 was first estimated by the empirical relation proposed by Viggiani & Atkinson (1995) for a normally consolidated clay characterised by a plasticity index $I_P = 20\%$

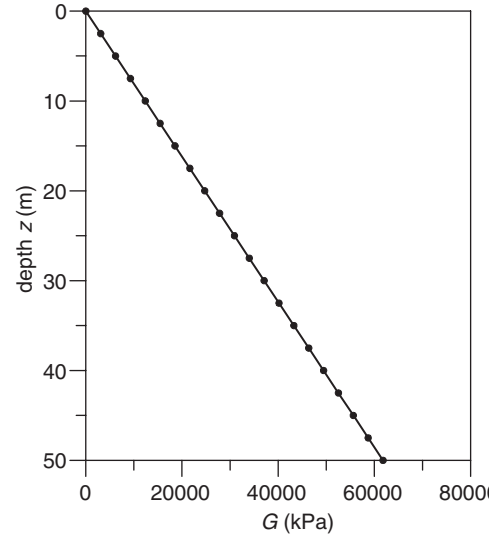

Figure 2. Profile of G assumed in the numerical analyses.

and then scaled down by a factor of 0.45 to account for the expected average shear strain level involved in the excavation stages $\bar{\gamma} = 0.1\%$. The parameter α was then defined by the best fit of the theoretical formulation against the empirical curve G-p in the range $0 < p < 200$ kPa. The corresponding initial profile of G with depth assumed for all the analyses is shown in Figure 2.

The bi-log compressibility index $\tilde{\lambda}$ was given a value compatible with what typically indicated in the literature for soft clays. A similar approach was adopted for the definition of the critical state parameter M.

The ratio ξ_s/η_s was kept constant to ensure that in all the analyses C it was only the rate of the de-structuring process to be modified but not its intensity (Amorosi & Boldini, 2003).

In all the numerical analyses an initial value of $K_0 = 0.57$ was adopted.

4 NUMERICAL RESULTS AND COMPARISON WITH EMPIRICAL SOLUTIONS

4.1 *Empirical solutions*

It is well known that in free field conditions the settlement trough related to tunnelling is well described by the Gaussian error function. The trough parameter i results to be a function of the tunnel depth z_0 by a factor K, which depends, among others, on depth and soil type. For soft clay at ground surface it varies between 0.6 and 0.7.

In order to get for soft clays a variation of K with depth similar the one proposed by Mair et al. (1993)

Copyright © 2006 Taylor & Francis Group plc, London, UK

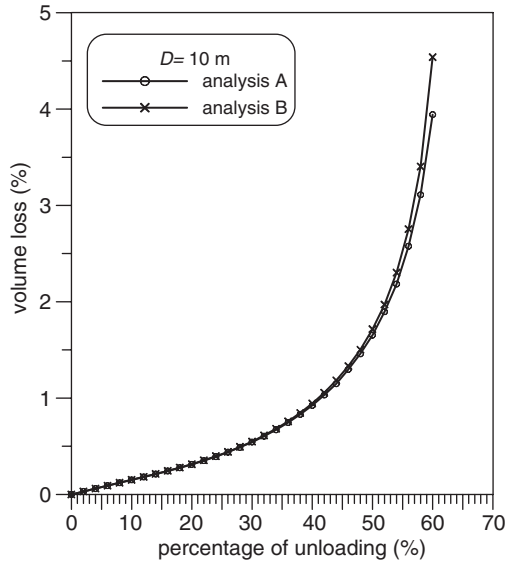

Figure 3. Numerical results: analyses A and B. Volume loss against percentage of unloading.

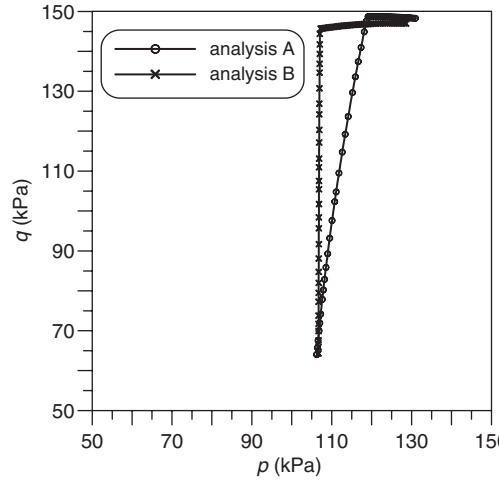

Figure 4. Numerical results: analyses A and B. Typical stress paths of Gaussian points located near the tunnel section (analysis A: $x = 10.11$ and $z = 14.89$; analysis B: $x = 10.27$ and $z = 14.96$).

for stiff clays, the following function is adopted in this study for the sub-surface settlement:

$$i = \mathrm{K}z_0 = \left[c_2 + \frac{c_1}{1 - \dfrac{z}{z_0}} \right] z_0 \qquad (7)$$

setting $c_2 = 0.525$ and $c_1 = 0.175$.

4.2 *Numerical results: analyses A and B*

Figure 3 shows the values of volume loss obtained for increasing percentage of unloading in analyses A and B. In both cases the curves indicate an initial linear trend followed by a non-linear one for unloading larger than about 30%. The collapse of the tunnel is achieved for unloading in excess of 60%.

The curves overlap up to an unloading of about 40%, corresponding to a volume loss slightly lower than 1%. For larger values of unloading, analysis B predicts slightly more significant volume losses than A.

Figure 4 shows two typical stress paths obtained in the two analyses for the same stress point. For initial states inside the yield surface and slightly dry of critical due to the presence of structure (i.e. enlarged yield surface) a parabolic elastic undrained stress path is predicted by analysis A. The standard $p =$ constant stress path characterizes the corresponding response of analysis B. It is worth noting that, although the undrained stress paths followed in the two analyses can be different from the very early stage of the excavation, the global responses shown in Figure 3 practically coincide up to a relatively large level of unloading.

Figure 5 shows the surface settlements for the two values of the volume loss. Again, no appreciable differences emerge between the results of analyses A and B for both values of the volume loss. The maximum settlements calculated in the numerical analyses A and B for a volume loss of 0.75% underestimate those predicted by the Gaussian distributions corresponding to $\mathrm{K} = 0.6$ and $\mathrm{K} = 0.7$. In addition, the settlements predicted by the numerical analyses produce wider subsidence profiles than those associated with the Gaussian distributions.

The accordance between the numerical results and the empirical predictions improves in the case of $V_L = 3.5\%$: the predicted maximum surface settlements are close to the one estimated by the Gaussian distribution for $\mathrm{K} = 0.6$. The comparison between the profiles of the empirical and numerical solutions shows that these latter produce narrower subsidence profiles but non-zero values of the settlements far from the tunnel axis of symmetry. Similar comments can be made for the sub-surface settlements at the depth of $z = 10$ m (Fig. 6).

In the following the predicted surface and sub-surface settlement curves obtained in the analyses are compared for the same values of volume loss, namely 0.75% and 3.5%. These two volume losses were selected as 0.75% is considered typical for a good performing EPB excavation while 3.5% is closer to the failure conditions for the problem under study.

Copyright © 2006 Taylor & Francis Group plc, London, UK

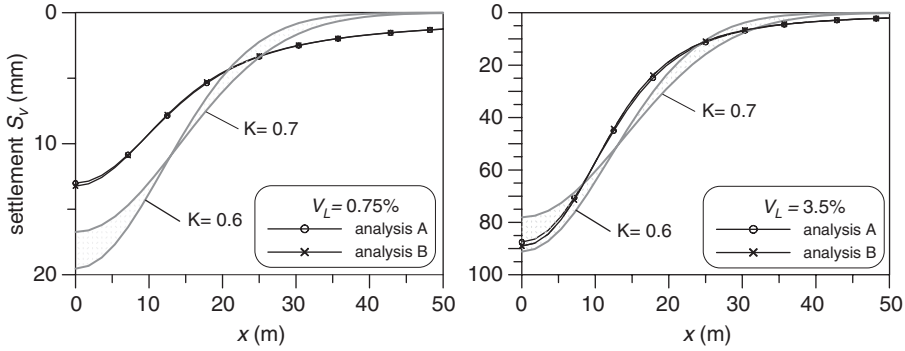

Figure 5. Numerical results: analyses A and B. Vertical settlement for a volume loss of 0.75% (on the left) and 3.5% (on the right).

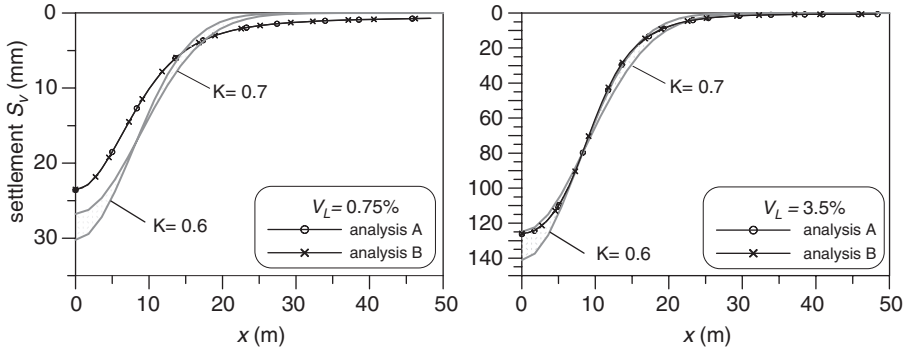

Figure 6. Numerical results: analyses A and B. Vertical displacement at z = 10 m for a volume loss of 0.75% (on the left) and 3.5% (on the right).

A volume loss of 0.75% is obtained in analyses A and B applying an unloading equal to 36.08% and 35.78%, respectively. The corresponding percentages of unloading to achieve a volume loss of 3.5% are equal to 59.09% and to 58.23%, respectively.

4.3 *Numerical results: analyses C1, C2, C3 and C4*

Figure 7 shows the calculated volume loss as a function of the percentage of unloading obtained in the four analyses C1-4.

Numerical results almost coincide up to a percentage of unloading of about 25%. For larger values, slightly increasing volume losses are obtained for in-creasing values of the destructuration parameters, when compared with reference to the same percentage of unloading.

The most important effect of the activation and increase of the de-structuring parameters consists in the reduction of the maximum percentage of unloading which can be achieved prior to the collapse of the ideal tunnel. In fact, none of the numerical results

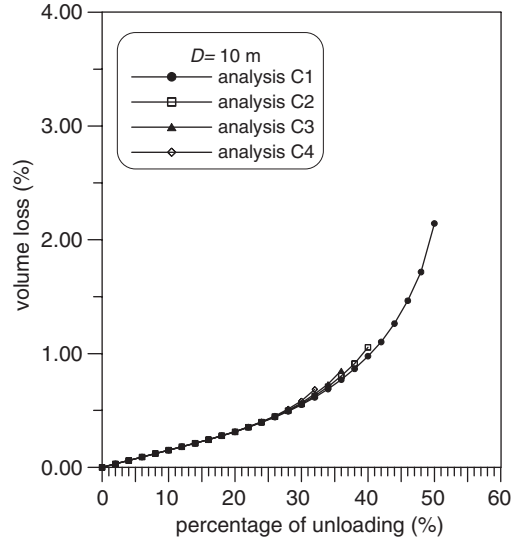

Figure 7. Numerical results: analyses C1, C2, C3 and C4. Volume loss against percentage of unloading.

Copyright © 2006 Taylor & Francis Group plc, London, UK

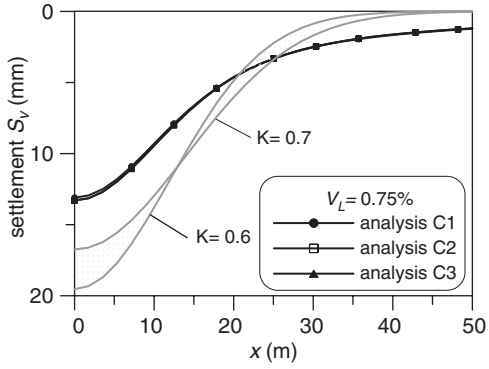

Figure 8. Numerical results: analyses C1, C2, and C3. Vertical settlement for a volume loss of 0.75%.

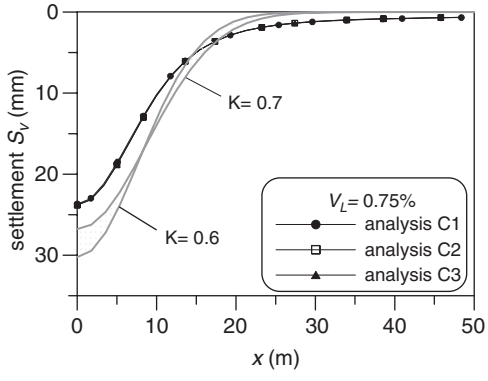

Figure 9. Numerical results: analyses C1, C2, and C3. Vertical displacement at z = 10 m for a volume loss of 0.75%.

reached the volume loss of 3.5%. Analysis C4 did not even achieved the volume loss of 0.75% as tunnel collapse occurred prior to this value. This volume loss was attained for percentages of unloading equal to 35.50, 34.94 and 34.33 in analyses C1, C2 and C3, respectively.

The surface and sub-surface settlement profiles predicted by the analyses where structure degradation is accounted for are shown in Figures 8 and 9. They do not differ significantly from those evaluated by analyses A and B for a volume loss equal to 0.75%: larger destructuration parameters only produce a small increment of the maximum settlement at $x = 0$.

5 CONCLUSIONS

In this paper the excavation of an ideal tunnel in a soft structured clay deposit is analysed numerically focusing on the induced surface and sub-surface settlements. The scope of this parametric study was that of separately establishing the relevance of the stress-induced anisotropy and that of the de-structuring processes on the tunnelling induced ground deformation for free field conditions. The behaviour of the soil was described by a Cam-Clay family single surface constitutive model, capable of reproducing stress-induced anisotropy by means of an isotropic hyperelastic formulation and plastic strain-driven structure degradation by an appropriate isotropic hardening law. An implicit stress point integration scheme was adopted to minimize the possible numerical inaccuracies which might have affected the overall response of this boundary value problem. The constitutive parameters and the initial conditions for the soil were selected with reference to the typical behaviour of natural structured clays while the imposed volume losses were those expected in both good or poorly performing EPB tunnel excavations.

The results of the analyses indicate that for the shallow tunnel under study the activation of the stress-induced anisotropy influences only marginally the settlement troughs. This outcome can be related to the moderate stress-induced anisotropy predicted by the proposed hyperelastic formulation for the selected parameters. Different conclusions were proposed by Einav & Puzrin (2004) which analysed an ideal shallow tunnel adopting a set of similar constitutive assumptions. This discrepancy might be attributed to the different criteria adopted in the two works to select the initial conditions and the constitutive parameters for the soil. In fact, these ingredients seems to play a role which is at least as important as that related to the constitutive assumptions themselves.

The de-structuring process influences the stability of the tunnel but, for relatively small values of the volume loss (= 0.75%), it results in a negligible effect in terms of settlement profiles. This should be related to the limited portion of the mesh undergoing significant plastic strain for such a small value of the volume loss.

Finally, it should be remarked that the conclusions drown above were obtained assuming a relatively simple constitutive model and, as such, should be generalised with some caution. In fact, further research is still needed in this field to investigate the influence of a number of other constitutive aspects, including: alternative hyperelastic potentials possibly accounting for intrinsic anisotropy, elasto-plastic coupling, diffuse plasticity (e.g.: bounding surface or multisurface formulations), plastic anisotropy and non-coaxiality.

REFERENCES

Amorosi, A & Boldini, D. 2003. Single surface hardening plasticity model for soft clays: mathematical formulation and implicit numerical integration. In Vermeer et al. (eds), *Constitutive modelling and analysis of boundary value problems in geotechnical engineering; Proc. Int. Work.*, *Noordwijkerhout*, 153–158.

Copyright © 2006 Taylor & Francis Group plc, London, UK

Amorosi, A, Boldini, D. & Germano, V. 2004. Single surface hardening plasticity model for soft clays: mathematical formulation and implicit numerical integration. *Plaxis meeting on user-defined soil models. Oral presentation, Karlsruhe, 13 November 2004.*

Borja, R.I., Tamagnini, C. & Amorosi, A. 1997. Coupling plasticity and energy-conserving elasticity models for clays. Journal of Geotechnical and Geoenvironmental Engineering, 123(10): 948–957.

Einav, I. & Puzrin, A.M. 2004. Pressure-dependent elasticity and energy conservation in elastoplastic models for soils. *Journal of Geotechnical and Geoenvironmental Engineering*, 130(1): 81–92.

Houlsby, G.T. 1095. The use of variable shear modulus in elastic-plastic models for clays. *Computers and Geotechnics*, 1: 3–13.

Jâky, J. 1994. The coefficient of earth pressure at rest. *Journal of the Union of Hungarian Engineers and Architects*, 355–358.

Kavvadas, M. & Amorosi, A. 2000. A constitutive model for structured soils. *Géotechnique* 50(3): 263–273.

Lee, K.M. & Rowe, R.K. 1990. Finite element modelling of the three-dimensional ground deformations due to tunnelling in soft cohesive soils: part II – results. *Computers and Geotechnics* 10: 111–138.

Mair, R.J., Taylor, R.N. & Bracegirldle, A. 1993. Subsurface settlement profiles above tunnels in clays. *Géotechnique* 43(2): 315–320.

Ortiz, M. & Popov, E.P.1985. Accuracy and stability of integration algorithms for elastoplastic constitutive relations. *International Journal for Numerical and Analytical Methods in Engineering* 21(9): 1561–1576.

Simpson, B., Atkinson, J.H. & Jovičić, V. 1996. The influence of anisotropy on calculations of ground settlements above tunnels. In Mair & Taylor (eds), *Geotechnical aspects of underground construction in soft ground, Proc. Int. Symp., London*, 591–594.

Viggiani, G. & Atkinson, J.H. 1995. Stiffness of fine-grained soils at very small strains. *Géotechnque*, 45(2): 249–265.

Copyright © 2006 Taylor & Francis Group plc, London, UK